Rab14 regulation of claudin-2 trafficking modulates epithelial permeability and lumen morphogenesis

Ruifeng Lu, Debra L. Johnson, Lorraine Stewart, Kelsey Waite, David Elliott, and Jean M. Wilson
Department of Cellular and Molecular Medicine, University of Arizona College of Medicine, Tucson, AZ 85724

ABSTRACT **Regulation of epithelial barrier function requires targeted insertion of tight junction proteins that have distinct selectively permeable characteristics. The insertion of newly synthesized proteins and recycling of internalized tight junction components control both polarity and junction function. Here we show that the small GTPase Rab14 regulates tight junction structure. In Madin–Darby canine kidney (MDCK) II cells, Rab14 colocalizes with junctional proteins, and knockdown of Rab14 results in increased transepithelial resistance. In cells without Rab14, there are small changes in the trafficking of claudin-1 and occludin. In addition, there is substantial depletion of the leaky claudin, claudin-2, but not other tight junction components. The loss of claudin-2 is complemented by inhibition of lysosomal function, suggesting that Rab14 sorts claudin-2 out of the lysosome-directed pathway. MDCK I cells lack claudin-2 endogenously, and knockdown of Rab14 in these cells does not result in a change in transepithelial resistance, suggesting that the effect is specific to claudin-2 trafficking. Furthermore, leaky claudins have been shown to be required for epithelial morphogenesis, and knockdown of Rab14 results in failure to form normal single-lumen cysts in three-dimensional culture. These results implicate Rab14 in specialized trafficking of claudin-2 from the recycling endosome.**

Monitoring Editor
Keith E. Mostov
University of California, San Francisco

Received: Dec 11, 2013
Revised: Mar 25, 2014
Accepted: Mar 25, 2014

INTRODUCTION

Epithelial cells form a barrier between the outside world and the interior of the organism. To establish this barrier, the cells develop discrete apical and basolateral membrane domains separated by specialized junctions. These junctions are selectively permeable, allowing some ions and macromolecules to pass through the epithelial barrier but excluding pathogens. Normal morphogenesis of epithelia depends on an array of interacting machineries: 1) the extracellular matrix, which provides directionality signals (O'Brien *et al.*, 2001; Yu *et al.*, 2005; Akhtar and Streuli, 2013); 2) the polarity complexes, comprising the Par3/Par6/aPKC complex, the Crumbs complex, and the Scribble/Lgl/Dlg complex, which promote separation of membrane domains and the establishment of tight junctions (Schluter *et al.*, 2009; Pieczynski and Margolis, 2011; Thompson, 2013); 3) the tight junctions, which serve as organizing and signaling centers both through the action of polarity complexes and their own structural components (Shin *et al.*, 2006); and 4) targeted membrane trafficking to both apical and basolateral domains, as well as to the tight junction (Apodaca *et al.*, 2012). These domains are not static, and our understanding of the dynamic nature of polarity and tight junctions has been enhanced by the recognition that these complexes undergo constant remodeling. In particular, tight junction proteins continuously cycle through endosomal compartments to maintain epithelial integrity (Marzesco *et al.*, 2002; Ivanov *et al.*, 2005; Morimoto *et al.*, 2005; Marchiando *et al.*, 2010; Shen, 2012).

Both polarized targeting of membrane proteins and recycling of tight junction proteins are regulated, in part, by the Rab family of small GTPases. Rab14 targets molecules to the apical plasma membrane (Kitt *et al.*, 2008), and Rabs 8, 11, and 13 regulate trafficking of junctional and adhesion molecules (Marzesco *et al.*, 2002; Kohler *et al.*, 2004; Lock and Stow, 2005; Morimoto *et al.*, 2005; Yamamura *et al.*, 2008; Roeth *et al.*, 2009; Momose *et al.*, 2011; Lapierre *et al.*, 2012). In addition, Rabs 8, 11, and 25 target vesicles to forming

This article was published online ahead of print in MBoC in Press (http://www.molbiolcell.org/cgi/doi/10.1091/mbc.E13-12-0724) on April 2, 2014.
Address correspondence to: Jean M. Wilson (jeanw@email.arizona.edu).
Abbreviation used: TER, transepithelial resistance.

luminal membranes, and disruption of these molecules results in aberrant morphogenesis in three-dimensional culture.

In addition to polarity and tight junction complexes, morphogenesis of epithelial organs requires that the epithelium be selectively permeable to ions and macromolecules. Selective permeability of the epithelium is essential for the function of the established epithelium (Anderson and Van Itallie, 2009) and also for initial lumen formation (Bagnat *et al.*, 2007). In particular, the presence of a class of claudin molecules that promote paracellular permeability is essential for normal lumen formation both in vitro and in vivo (Bagnat *et al.*, 2007; Galvez-Santisteban *et al.*, 2012), and regulation of levels of other claudins also plays a role in the regulation of lumen size (Senga *et al.*, 2012). However, how these claudins are regulated to promote normal epithelial morphogenesis is not known. Here we show that knockdown of Rab14 results in loss of the "leaky" claudin, claudin-2, decreased paracellular permeability, and failure of normal epithelial morphogenesis.

RESULTS

Rab14 knockdown results in higher transepithelial resistance

MDCK II cells were infected with lentiviral vectors expressing two independent short hairpin RNAs (shRNAs) within the Rab14 coding sequence (E9 and E11) and selected to generate stable knockdown cell lines. Both shRNAs provided knockdown of Rab14 protein (Figure 1, A and B), with clone E9 providing >60% knockdown. This clone was used for the present experiments, and knockdown was reconfirmed throughout the course of the experiments. Of interest, knockdown of Rab14 resulted in higher transepithelial resistance (TER) at steady state, and increase in TER was correlated with degree of Rab14 knockdown (Figure 1C). Furthermore, expression of the GTP- or GDP-locked forms of Rab14 (Rab14-Q70L or Rab14-S25N) also resulted in increased steady-state TER (Supplemental Figure S1). These results are consistent with other junction-associated small GTPases, where fine control of activation/inactivation is required for normal junction assembly and function (Rojas *et al.*, 2001; Bruewer *et al.*, 2004; Yamamura *et al.*, 2008; Elbediwy *et al.*, 2012). These results suggest that Rab14 regulates tight junction function.

Rab14 colocalizes with tight junction proteins

In polarized epithelial cells, Rab14 is localized to the apical endosomes but is not concentrated at the lateral membrane or at tight junctions (Kitt *et al.*, 2008). To assess the relationship between Rab14 and tight junction proteins, we studied the localization of endogenous Rab14 and claudin-2, claudin-4, and occludin in MDCK cells by confocal microscopy. In addition, due to antibody incompatibility, we localized claudin-1 in cells expressing Rab14–green fluorescent protein (GFP). There is colocalization of Rab14 and claudin-2 and -4 in intracellular puncta (Figure 1D, top) and Rab14-GFP with claudin-1 (Figure 1D, bottom). However, colocalization of occludin and Rab14 was not detected. In addition, there is colocalization of Rab14-GFP and claudin-1, -2, and -4 near the lateral membranes in cells grown on Transwell filters (Supplemental Figure S2). It is important to note that, even under overexpressed conditions, Rab14-GFP constitutes <30% of the total Rab14 expressed in these cells (Supplemental Figure S3). Both Rab13 and Rab11 were implicated in the trafficking of tight junction and adherens junctions proteins (Marzesco *et al.*, 2002; Lock and Stow, 2005; Morimoto *et al.*, 2005; Desclozeaux *et al.*, 2008; Roeth *et al.*, 2009; Lapierre *et al.*, 2012), but limited colocalization of claudin-1 was observed with either Rab11-GFP or Rab13-GFP (Supplemental Figure S1).

Rab14 modulates assembly of tight junctions

To determine whether Rab14 modulates assembly of tight junctions, we subjected cells plated on Transwell filters to calcium switch by incubation in calcium-free medium overnight, followed by replacement with normal calcium-containing medium (Gumbiner *et al.*, 1988). Monolayers were fixed at intervals and labeled with antibodies against junction proteins, followed by imaging through the entire monolayer. The formation of junctions occurs through well-characterized stages of adhesion and maturation, and a continuous, compact line around the cell perimeter characterizes mature junctions (Wallace *et al.*, 2010; Iden *et al.*, 2012). To quantify junction assembly, we measured the width of labeling at the junction (claudin-1) or the percentage of lateral membrane occupied by tight junction label (occludin) as detailed in *Materials and Methods*. Of interest, cells with depleted Rab14 had accelerated restoration of claudin-1 distribution to the junction, as mature junctions formed more quickly than control cells (Figure 2A). This difference was most apparent 2 h after calcium switch. In addition, junctional labeling of occludin was largely restored within 1 h after the switch to normal growth medium in Rab14-knockdown (KD) cells but was slower in control cells (Figure 2, D and E). E-cadherin labeling was also restored at earlier time points than for control cells (Figure 2F). These results suggest that, in addition to modulating adherens junction formation (Linford *et al.*, 2012), Rab14 modulates trafficking of tight junction proteins through either decreased internalization or increased recycling of these components. To test this, we performed cell surface biotinylation internalization and recycling assays. For these experiments, cells were biotinylated and warmed for 10 min to allow internalization and cooled, and cell surface label was removed with 2-mercaptoethane sulfonate (MESNA). NeutrAvidin precipitation brings down label that is protected from MESNA and thus is the internalized pool. As shown in Figure 3, there is no difference in the amount of occludin internalized in Rab14-KD and control cells (Figure 3, A and B). However, less claudin-1 is internalized in Rab14-KD cells (Figure 3, A and C). To measure recycling, we rewarmed cells after MESNA treatment for an additional 10 min, followed by MESNA treatment to remove recycled biotin. NeutrAvidin precipitation retrieves the remaining biotinylated proteins, and these biotinylated proteins were subtracted from the internalized pool to quantify recycled occludin and claudin-1. As shown in Figure 3, B and C, both occludin and claudin-1 were recycled slightly but significantly faster in Rab14-KD cells.

Rab14 depletion decreases the protein levels of the tight junction protein claudin-2

Although the calcium switch and biotinylation assays suggested small changes in trafficking of junctional proteins, it seems unlikely that these changes account for the increased TER observed in Rab14-KD cells. To determine whether Rab14-KD affects the steady-state distribution of tight junction proteins, we labeled MDCK cells grown on Transwell filters with antibodies against the tight junction membrane proteins occludin and claudin-1 and -4, as well as against the adhesion junction protein E-cadherin. As shown in Figure 4, the distribution of E-cadherin, occludin, claudin-1, and ZO-1 is not altered with Rab14 knockdown. To determine whether the protein level of any of these junctional components is changed after Rab14-KD, we analyzed cell lysates by Western blotting to assess total levels of junction proteins. The amounts of claudin-1 and -4, occludin, and ZO-1 are unchanged (Figure 5A). However, the level of claudin-2 is significantly decreased (Figure 5, A and B). Immunolabeling of Rab14-KD cells shows a substantial loss of claudin-2 labeling at the junctions (Figure 5C). To confirm that the loss of claudin-2 is due

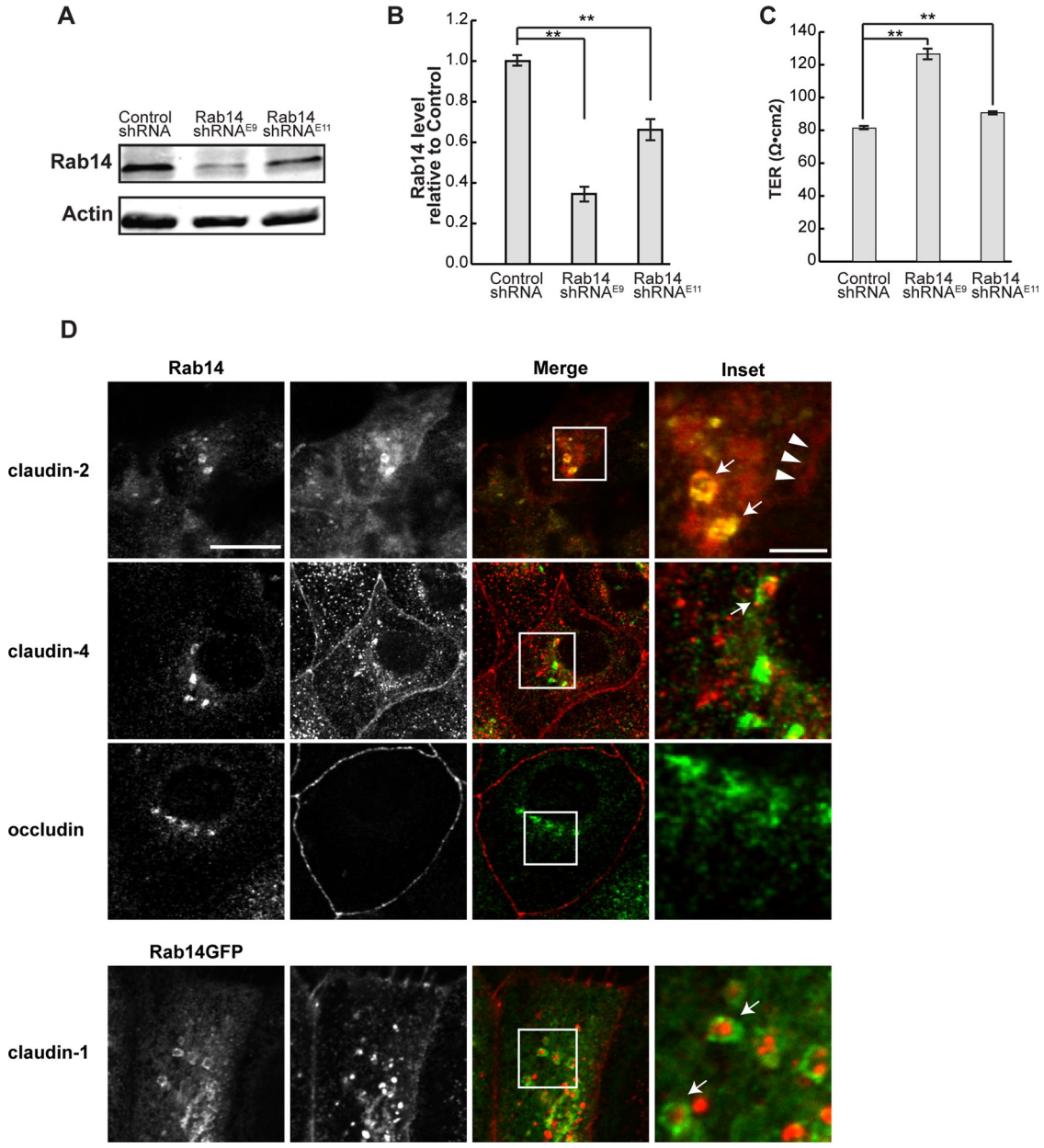

FIGURE 1: Rab 14 knockdown results in higher transepithelial resistance. (A) MDCK II cells were infected with lentiviral vectors encoding two independent shRNA sequences (Rab14shRNA^{E9} or Rab14shRNA^{E11}) or scrambled sequence. Cell lysates were analyzed by Western blotting and probed with Rab14 antibody. β-Actin was used as a loading control. (B) Quantification of Rab14 levels shows knockdown, with E9 providing greater knockdown ($n = 5$). (C) The TER of monolayers is increased with Rab14 knockdown, with cells with greater knockdown exhibiting a greater increase in TER ($n = 2$ in triplicate, mean ± SEM, $^{**}p < 0.001$). (D) Endogenous Rab14 (top) or Rab14-GFP (bottom) colocalizes with claudins. Rab14 and claudin-1, -2, and -4 colocalize in intracellular vesicles (arrows), but there is limited colocalization with occludin. Claudin-2 at the lateral membrane is indicated by arrowheads. Scale bar, 10 μm; inset, 2 μm.

to Rab14 knockdown, we overexpressed an shRNA-resistant form of Rab14 and quantified the level of claudin-2. As shown in Figure 5D, reexpression of Rab14 largely complemented the loss of claudin-2.

To determine whether decreased claudin-2 is a result of increased lysosomal degradation, we incubated Rab14-KD cells with ammonium chloride for 24 h, as this lysosomotropic agent raises the pH of lysosomal compartments, inhibiting the action of the acid proteases. Under these conditions, claudin-2 levels increased (Figure 6, A and B). Of interest, control cells show a substantial increase in claudin-2, indicating that it is normally rapidly trafficked to lysosomes. Immunolabeling of these cells with claudin-2 and Lamp1 antibodies shows that some claudin-2 colocalizes with Lamp1-positive puncta (Figure 6C). Given that claudin-2 acts to increase permeability across epithelia, these results suggest that the higher TER observed in Rab14-KD cells is due to loss of claudin-2 and that Rab14 normally functions to sort claudin-2 out of the lysosomal pathway.

To further test whether the effects of Rab14 knockdown on TER are due to claudin-2 loss, we next overexpressed human claudin-2 in Rab14-KD cells. As shown in Figure 7A, we can overexpress claudin-2 in the Rab14-KD background and restore claudin-2

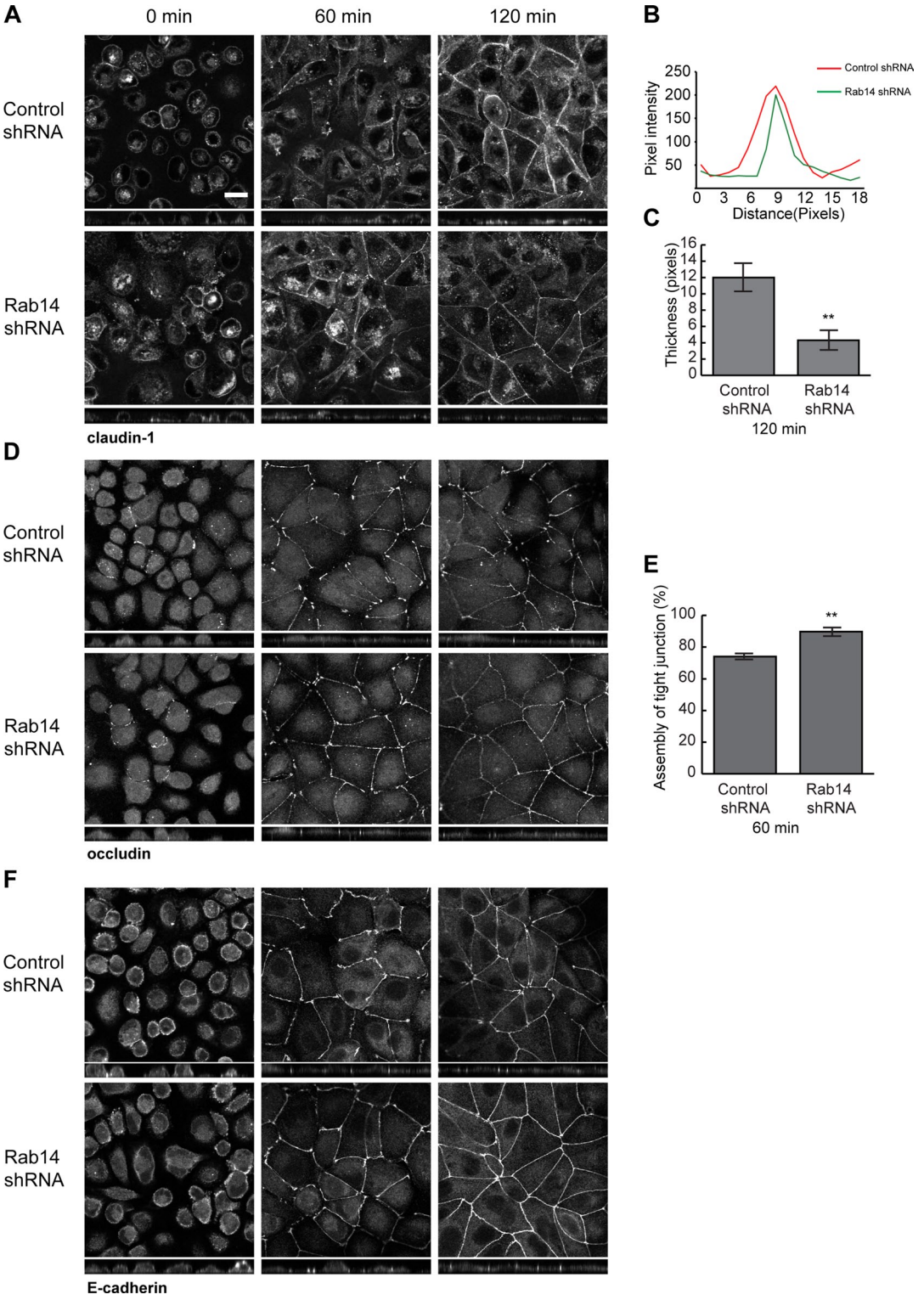

FIGURE 2: (A) Rab14-KD cells form junctions more rapidly after calcium switch. Cells on Transwell filters were incubated in calcium-free medium overnight, and then normal growth medium was replaced for the indicated intervals followed by fixation and labeling with the antibodies indicated. Cells were imaged through the *Z*-axis, and the images presented are projections of the *Z*-stack. Quantification was performed as described in *Materials and Methods*. Rab14-KD cells had faster maturation of claudin-1 labeling when compared to control cells, as assessed by the width of labeling, with mature junctions exhibiting compact, continuous labeling (A–C). In B, pixel intensity of 50 was used as baseline, and higher pixel values were considered part of the junction. Values were graphed across the junction width, and a representative profile is shown. In C, junction thickness was measured across pixel intensity values above 50 and resulting widths were averaged. (D, E). Occludin is targeted back to the lateral membrane more quickly in Rab14-KD cells as measured by percentage of the lateral membrane occupied by occludin labeling (n = 250 cells, mean + SEM). (F) E-cadherin is also targeted to the lateral membrane more quickly in Rab14-KD cells. Scale bar, 10 μm.

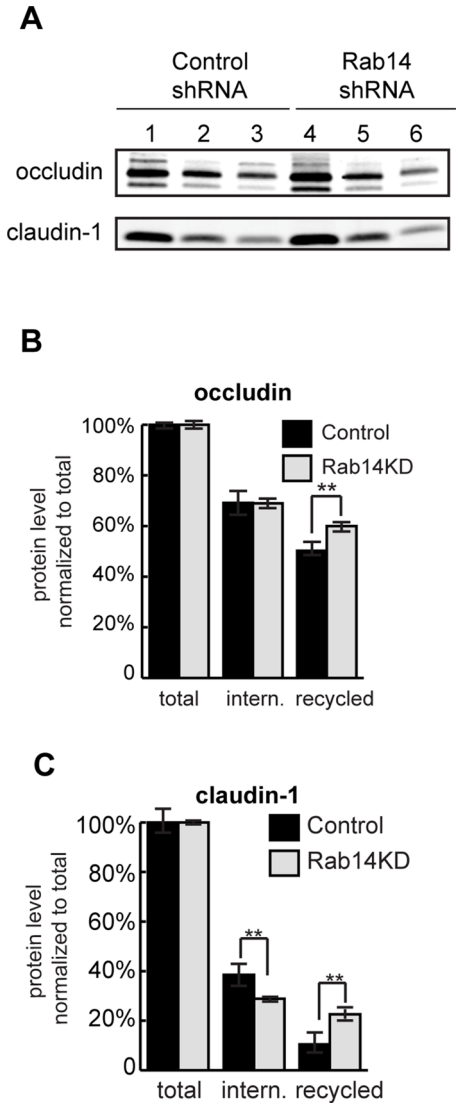

FIGURE 3: Surface biotinylation internalization and recycling assays of Rab14 knockdown cells. (A) Cells were biotinylated and immediately lysed (lanes 1 and 4) or incubated at 37°C for 10 min (lanes 2 and 5), followed by cell surface stripping with MESNA and NeutrAvidin precipitation. In lanes 3 and 6, cells were warmed for an additional 10 min after MESNA stripping to allow recycling, followed by MESNA stripping. Internalization was quantified by calculating the ratio of internalized (lanes 2 and 5) over total (lanes 1 and 4). Recycling was calculated by subtracting the biotinylated protein remaining after rewarming (lanes 3 and 6) from the internalized pool (lanes 2 and 5). (B) Quantification shows that occludin is taken up similarly in knockdown and control cells. However, recycling of occludin is faster in Rab14-KD cells. (C) Claudin-1 is internalized more slowly and recycles more quickly in Rab14-KD cells. $^{**}p < 0.001$; $n = 3$, mean ± SEM.

expression. Under these conditions, the TER is complemented, bringing it down to control levels (Figure 7B). In addition, imaging shows that overexpressed human claudin-2 localizes to junctions (Figure 7C). Normal initial targeting of claudin-2 under these conditions suggests that Rab14 regulates endosomal recycling of claudin-2 rather than targeting from the *trans*-Golgi network. Furthermore, overexpression of an shRNA-resistant form of Rab14-GFP results in complementation of the increased TER and claudin-2 presence at junctions (Figure 7, B and C).

To further test whether the observed change in TER is due to loss of claudin-2, we used MDCK I cells. Claudin-2 is not expressed in MDCK I (Furuse *et al.*, 2001), which is believed to contribute to the high TER of this strain. MDCK I cells were infected with the two lentiviral vectors used in Figure 1 and selected to generate stable lines. Both shRNAs provided knockdown of Rab14 (Figure 8A). Of importance, knockdown of Rab14 does not result in a significant change in TER (Figure 8B), and there was no change in the subcellular distribution of claudin-1 or -4, occludin, or ZO-1 (Figure 8C). This result is consistent with the conclusion that the increase of TER in Rab14-KD MDCK II cells is due to the loss of claudin-2.

Rab14 regulates formation of epithelial cysts

Loss of claudin-2 has been shown to disrupt the development of epithelial cysts in three-dimensional (3D) culture (Galvez-Santisteban *et al.*, 2012), and a related claudin, claudin-15, is essential for lumen formation in zebrafish intestine (Bagnat *et al.*, 2007). To test whether Rab14-KD disrupted epithelial polarity or morphogenesis, we plated cells in 3D culture and analyzed the formation of epithelial cysts. Rab14-KD results in the formation of multilumen cysts (Figure 9, A and B), suggesting that epithelial morphogenesis is disrupted. Of interest, even with the multilumen phenotype, apical and basolateral markers are targeted to the correct membrane domain, and the Golgi apparatus maintains its supranuclear localization (Figure 9A).

DISCUSSION

Regulation of the internalization and recycling of tight junction proteins is essential to control of paracellular permeability and polarity. In this study, we sought to understand how the small GTPase Rab14 modulates tight junction structure and function through control of the trafficking of integral membrane components of these specialized domains. Rab14 is involved in multiple membrane-trafficking pathways, including targeting to the apical plasma membrane (Kitt *et al.*, 2008), phagolysosome biogenesis (Kyei *et al.*, 2006; Kuijl *et al.*, 2007), insertion of the glucose transporter GLUT-4 into the plasma membrane (Ishikura *et al.*, 2007), trafficking of the FGF receptor (Ueno *et al.*, 2011), and trafficking of ADAM proteases (Linford *et al.*, 2012). These reports, together with our finding that Rab14 selectively inhibits lysosomal targeting of claudin-2, suggest that Rab14 regulates trafficking of a subset of membrane proteins between specialized membrane domains.

Multiple Rab proteins have been shown to regulate both tight and adherens junctions. For example, Rab13 regulates trafficking of tight junction proteins (Marzesco *et al.*, 2002; Morimoto *et al.*, 2005), and knockdown of Rab13 decreases recycling of occludin and claudin-1, as does knockdown of the Rab13 effector JRAB/MICAL-L2 (Yamamura *et al.*, 2008). Rab25 depletion causes small effects on the expression of tight junction proteins (Krishnan *et al.*, 2013), and Rab8 and Rab11 regulate trafficking of E-cadherin (Lock and Stow, 2005; Yamamura *et al.*, 2008). Although Rab14 has been implicated in adherens junction assembly, this is due to effects on trafficking of ADAM proteases (Linford *et al.*, 2012) rather than on the trafficking of N-cadherin. We find that Rab14 colocalizes with several claudin proteins, and Rab14-KD results in faster reassembly of junctions after calcium switch. However, the effects of Rab14 knockdown on internalization, recycling, or steady-state distribution of claudin-1 and occludin were relatively small, in contrast to the nearly complete loss of claudin-2 expression. In addition, the lack of a phenotype after Rab14 knockdown in MDCK I cells, a strain that lacks endogenous claudin-2, suggests that Rab14 primarily controls claudin-2 trafficking rather than affecting the trafficking of tight junction proteins generally. These results suggest that Rab14 selectively

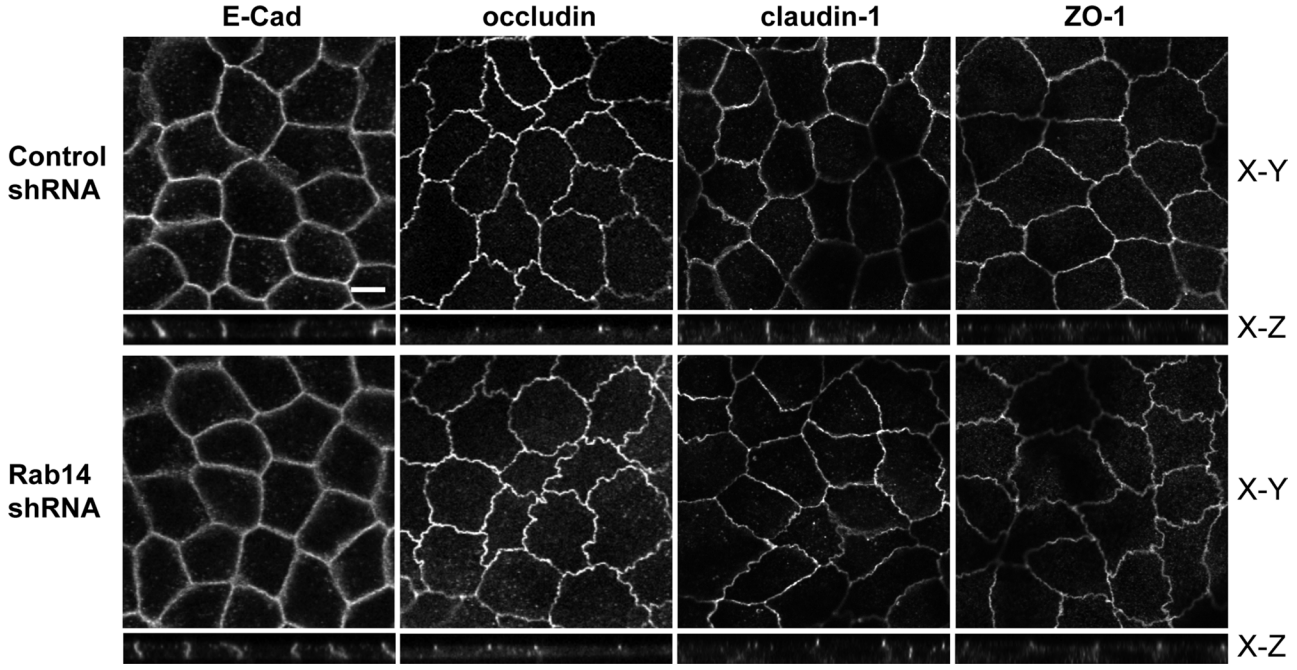

FIGURE 4: E-cadherin, occludin, claudin-1, and ZO-1 distributions are not affected when Rab14 is depleted. Rab14-KD and control cells were plated on Transwell filters and grown for 7 d, followed by fixation and labeling. Images were collected through the *z*-axis, and the brightest plane is illustrated in the *x-y* panels, with the *z*-plane below. The labeling of these junction proteins in Rab14-KD cells appears identical to control cells. Scale bar, 10 μm.

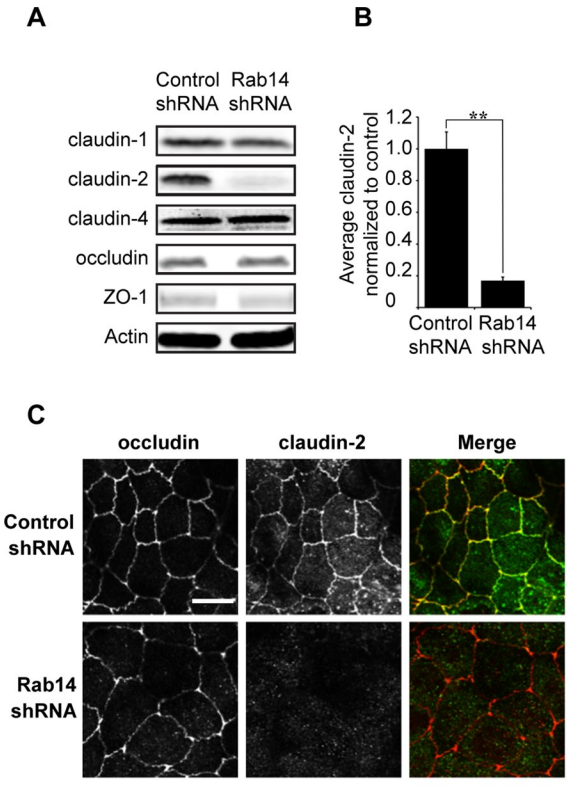

FIGURE 5: Claudin-2 levels are decreased in Rab14-knockdown cells. (A) Quantification of junction proteins in Rab14-KD cells. Claudin-2 levels are substantially decreased; this decrease is quantified in B. Other tight junction proteins are unchanged. (C) Cells grown on coverslips were labeled for occludin and claudin-2. Claudin-2 labeling is lost in Rab14-KD cells. (D) Overexpression of an shRNA-resistant Rab14 ($Rab14^R$) partially restores claudin-2 protein levels. Graphs represent one of multiple experiments done in triplicate (mean ± SEM, $^{**}p < 0.001$). Scale bar, 10 μm.

regulates recycling of claudin-2. Nonetheless, it may be that Rab14 also acts in opposition to Rab13 to promote recycling of claudin-1 and occludin from the endosomal compartment.

Claudin-2 forms cation-selective pores that increase paracellular permeability (Hou *et al.*, 2006). Transcription of claudin-2 is controlled by cytokines and growth factors (Amasheh *et al.*, 2010; Suzuki *et al.*, 2011), and internalization and recycling are regulated by the lipid kinase PIKfyve (Dukes *et al.*, 2012). Furthermore, phosphorylation on serine 208 reduces its trafficking to lysosomes (Van Itallie *et al.*, 2012). Although we do see decreased transcriptional levels of claudin-2 in Rab14-knockdown cells (unpublished data), our results suggest that regulation of lysosomal targeting by Rab14 is an important component of regulation of claudin-2 protein levels. Of interest, even in control cells, inhibition of lysosomal degradation resulted in higher expression of claudin-2, suggesting that claudin-2 is normally turned over quickly. Because claudin-2 is increased in inflammatory bowel disease (Zeissig *et al.*, 2007; Weber *et al.*, 2008), Rab14 may serve as an important regulator in the development of this pathology.

Normal epithelial morphogenesis requires interaction with the extracellular matrix, polarity complexes, and machinery for polarized targeting of apical and basolateral

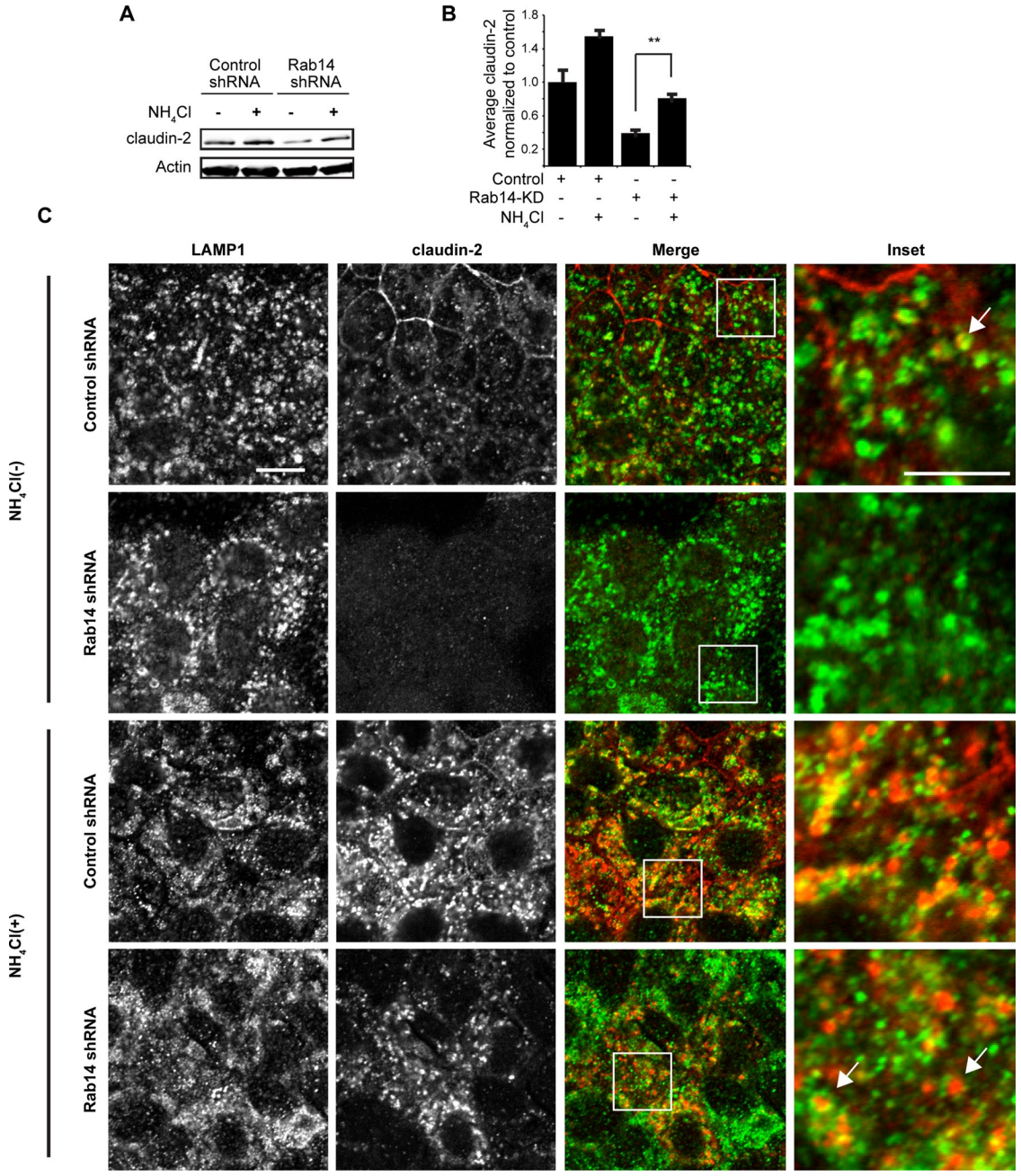

FIGURE 6: Ammonium chloride treatment restores claudin-2 protein levels. (A) Cells were incubated in medium containing 20 mM NH_4Cl and analyzed by Western blot. (B) Quantification of claudin-2 protein level shows that NH_4Cl treatment partially restores claudin-2 protein levels. Representative experiment performed three independent times. (C) Immunofluorescence of control and Rab14-KD cells shows that claudin-2 labeling is substantially increased after NH_4Cl incubation. In addition, some claudin-2 colocalizes with the lysosomal marker LAMP1 (arrows). Scale bar, 10 μm; inset, 5 μm.

membrane proteins (Datta *et al.*, 2011). Rab 27 and Rab3 initiate a single lumen to form cysts (Galvez-Santisteban *et al.*, 2012), and early events in cyst morphogenesis require Rab11a, Rab8a, and Rab25 (Bryant *et al.*, 2010). Loss of claudin-2 disrupts the development of epithelial cysts in 3D culture (Galvez-Santisteban *et al.*, 2012), and a related claudin, claudin-15, is essential for lumen formation in zebrafish intestine (Bagnat *et al.*, 2007). We show here that Rab14-KD results in the formation of multilumen cysts. Of interest, even with the multilumen phenotype, apical and basolateral markers are targeted to the correct membrane domains. Whereas Rab14 has been implicated in apical targeting of VIP/Mal, gp135/podocalyxin is normally targeted when Rab14 activity is disrupted (Kitt *et al.*, 2008). For cyst morphogenesis, it may be that the aberrant targeting of apical proteins and loss of claudin-2 expression combine to disrupt cyst formation.

We find that depletion of Rab14 causes a selective loss of claudin-2 from epithelial cells. We propose that Rab14 normally acts to retain claudin-2 in the recycling pathway, and failure of Rab14 to sort claudin-2 from endosomes to the junctional region results in targeting to lysosomes. We do not know whether Rab14 binds directly to

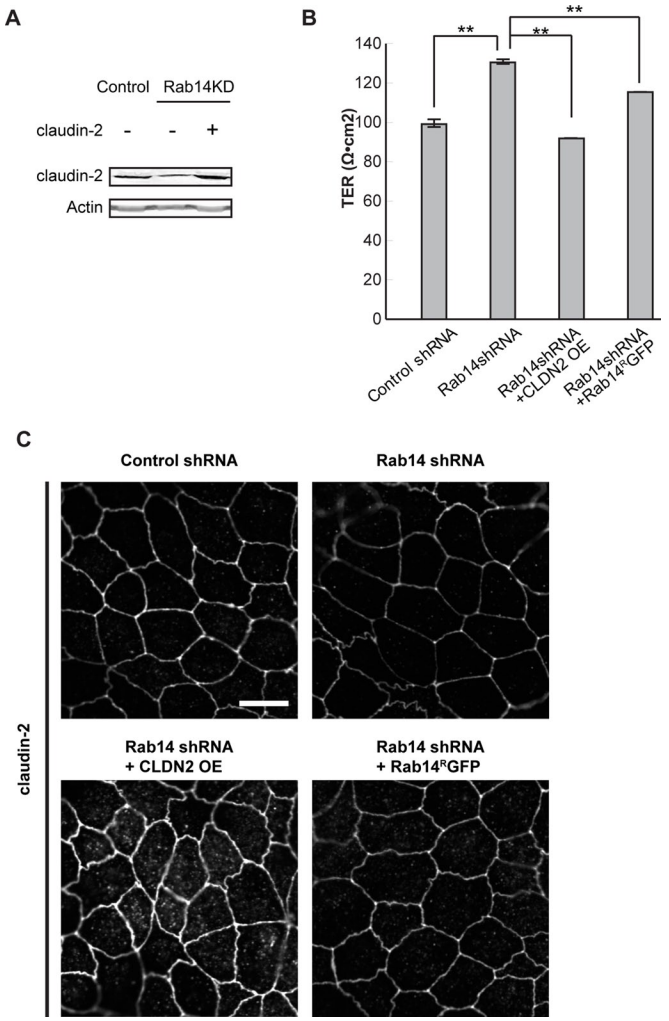

FIGURE 7: Expression of claudin-2 or shRNA-resistant Rab14 (Rab14^{R}GFP) complements the increased TER in Rab14-KD cells. (A) Rab14-KD or control cells were infected with a lentiviral vector encoding full-length human claudin-2 (CLDN2 OE). Western blot confirms overexpression of human claudin-2. (B) Overexpression of human claudin-2 or shRNA-resistant Rab14 in Rab14-KD cells results in decreased TER. Graph represents a single experiment performed in triplicate (**$p < 0.001$, mean ± SEM). (C) Monolayers were fixed and labeled with claudin-2 antibody. Overexpressed claudin-2 was correctly targeted to the junctional region, and overexpression of shRNA-resistant Rab14 results in increased claudin-2 at the junctions. Scale bar, 10 μm.

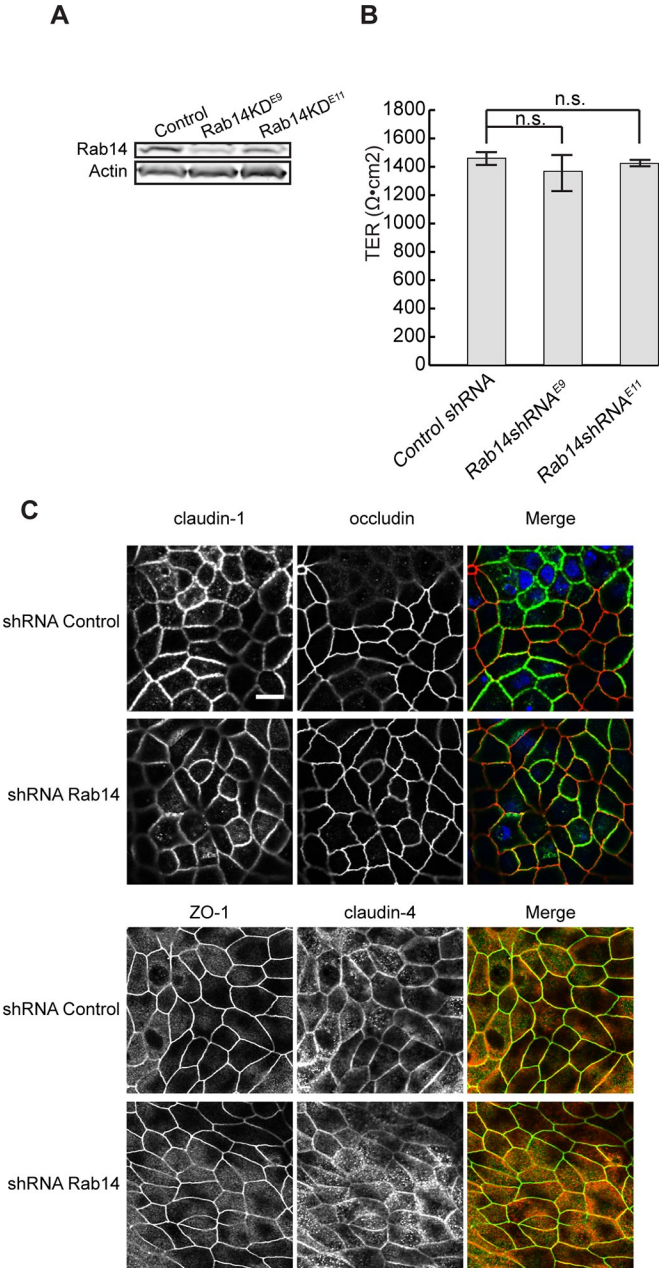

FIGURE 8: Depletion of Rab14 in high-TER MDCK I cells does not increase TER. (A) MDCK I cells were infected with the same lentiviral vectors as in Figure 1A. Cell lysates were analyzed by Western blotting and probed with Rab14 antibody. β-Actin was used as loading control. (B) Control and knockdown cells were plated on Transwell filters, and the TER was measured 7 d after plating. The TER is not significantly changed in Rab14-knockdown cells. Graph represents a single experiment performed in triplicate. n.s., not significant. (C) MDCK I control and Rab14-KD cells were fixed and labeled with tight junction markers. The distributions of occludin, claudin-1 and -4, and ZO-1 appear normal. Scale bar, 10 μm.

claudin-2 or whether the effects of Rab14 are mediated through other effectors, such as motor proteins. Future work will determine whether phosphorylation or other posttranslational modifications of claudin-2 modulate the effect of Rab14 on this trafficking.

MATERIALS AND METHODS

Materials

Cell culture reagents were obtained from Mediatech (Manassas, VA). The following antibodies were used: rabbit anti-Rab14 (AVIVA, San Diego, CA), rabbit anti-Rab14 (Sigma-Aldrich, St. Louis, MO), rat anti–E-cadherin (DECMA; Sigma-Aldrich), mouse anti-gp135 (gift from K. Matlin, University of Cincinnati, Cincinnati, OH), and rabbit anti–claudin-1, rabbit and mouse anti–claudin-2, mouse anti–claudin-4, and rabbit and mouse anti-occludin (all from Invitrogen, Grand Island, NY). Alexa Fluor secondary antibodies were also from Invitrogen. All other chemicals and reagents were from Sigma-Aldrich unless otherwise specified.

Plasmid/lentivirus constructs

pLKO-shRNAs Rab14 were a gift from the Broad Institute, Harvard Medical School. The following sequences are used for the knockdown of Rab14:

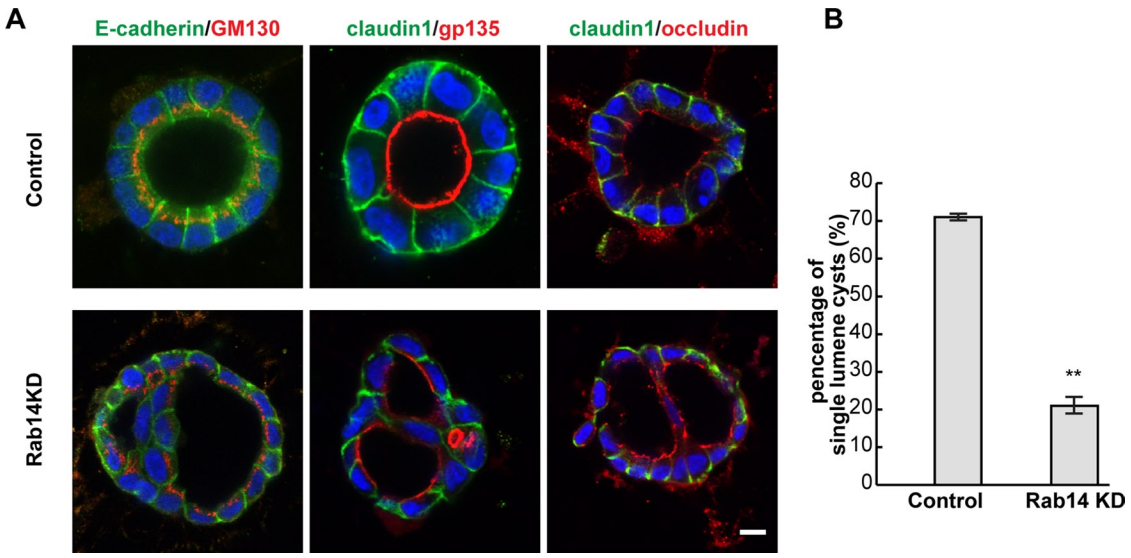

FIGURE 9: Rab14 knockdown impairs cyst formation. (A) Rab14-KD and control cells were plated in Matrigel and grown for 4 d, followed by labeling for apical and basolateral markers. The basolateral and junctional markers E-cadherin and claudin-1 maintain the correct localization, and the apical marker gp135 (podocalyxin) is targeted to the apical plasma membrane. However, knockdown of Rab14 results in the formation of multiple-lumen cysts. (B) Quantification of the percentage of single lumen cysts ($n > 200$, $^{**}p < 0.001$, mean ± SEM). Scale bar, 10 μm.

E9: GAAGCCAAACAGTTTGCTGAA

E11: GGTGTTGAATTTGGTACAAGA

Knockdown was confirmed and quantified by immunoblotting using anti-Rab14 antibody (see later description). Rab14-GFP plasmids were previously described (Kitt *et al.*, 2008). Relative expression levels of Rab14-GFP plasmids compared with endogenous Rab14 are illustrated in Supplemental Figure S3.

Cell culture

MDCK cells were used in all experiments, and the low-resistance MDCK II strain was used for the majority of experiments unless otherwise indicated. Cells were cultured in DMEM-High glucose (Mediatech) supplemented with 10% fetal bovine serum (FBS; Atlanta Biologicals, Lawrenceville, GA), 1% nonessential amino acids (Mediatech), and 1% Pen/Strept/L-Glut (Sigma-Aldrich) under 5% CO_2 at 37°C.

Cells were transfected using the Amaxa nucleofection system using solution T and setting P-029. Cells were selected with 400 μg/ml G418. For lentiviral transduction to knock down Rab14 expression, cells were infected in the presence of 6 μg/ml Polybrene (Sigma-Aldrich) overnight followed by selection in growth medium containing 2 μg/ml puromycin. Cells were maintained in growth medium with 2 μg/ml puromycin, and knockdown was confirmed throughout the course of the experiments.

For TER measurements, cells were plated at a density of 1.3×10^5 cells/cm^2 on filter inserts (3460; Corning, Corning, NY) and cultured for 4–5 d. TER was measured with a Millicell ERS-2 epithelial volt-ohm meter (Millipore, Billerica, VA). TER measurements are expressed as ohms·centimeter squared (Ω·cm^2). TER measurements were performed in triplicate.

For calcium switch experiments, cells were plated at 1×10^5/well on coverslips in a 24-well plate and grown to confluence. Cells were incubated in calcium-free medium (Spinner plus 10% dialyzed FBS) for 18–20 h, and loss of cell–cell contact was confirmed by phase microscopy. Regular calcium-containing medium was added, and cells were fixed at time points after medium change as indicated in the figures.

For ammonium chloride treatment, control and knockdown cells were incubated in medium containing 20 mM NH_4Cl for 24 h before lysis for Western blotting or fixation for immunofluorescence.

Immunofluorescence labeling and fluorescence microscopy

Cells were cultured on sterilized coverslips or Transwell filters as described. For imaging cells on filters, cells were plated at confluent density (2×10^5 cells/cm^2) cultured for 3–5 d. For immunofluorescence labeling, cells were fixed in 4% paraformaldehyde, permeabilized with 0.2% saponin/phosphate-buffered saline (PBS), and incubated in primary antibodies overnight at 4°C, followed by incubation with fluorescent secondary antibodies. Images were acquired using an Olympus FluoView confocal microscope (Olympus, Tokyo, Japan) with a 60× (numerical aperture 1.4) oil immersion objective. Excitation wavelengths of 488, 568, and/or 633 nm were used for simultaneous two- or three-channel recording. Images were processed and merged using Photoshop (Adobe, San Jose, CA) or ImageJ (National Institutes of Health, Bethesda, MD). For comparison, identical imaging and processing parameters were used in each experiment.

Tight junction quantification

For each sample, images were obtained at 60× magnification and tight junction formation quantified using ImageJ. For claudin-1 labeling, lines were drawn through the junction perpendicular to the lateral membrane and pixel intensity quantified. A pixel intensity of 50 was used as baseline, and higher values were considered part of the junction. Values were graphed across the junction width. Junction widths were then averaged. Maturation of occludin labeling was measured by percentage of the lateral membrane occupied by occludin labeling. By use of ImageJ, cell junctions were traced, and the ratio of occludin-positive junction over total junction length was calculated. Error bars are SEM.

Internalization and recycling assays

Cell surface biotinylation was accomplished using a reversible biotinylation kit (89881; Thermal Scientific, Rockford, IL). Cell surface proteins were biotinylated with 0.25 mg/ml Sulfo-NHS-SS-Biotin on ice for 30 min. Unbound biotin was quenched according to manufacturer instructions, and cells were then incubated at 37°C for 10 min to allow internalization of cell surface proteins. Cells were cooled to 4°C and washed three times with 100 mM MESNA in PBS and quenched with 5 mg/ml iodoacetimide. For internalization assays, cells were immediately lysed in RIPA buffer (20 mM Tris, 100 mM NaCl, 1% Triton, 1% Na-deoxycholate, 0.1% SDS). For recycling assays, cells were incubated at 37°C for 10 min, reduced, and lysed as described. Clarified cell lysates were incubated with NeutrAvidin agarose for 60 min at room temperature. Beads were washed with RIPA buffer before heating to 95°C for 5 min in SDS–PAGE sample buffer (62.5 mM Tris-HCl, pH 6.8, 1%SDS, 10% glycerol, 50 mM dithiothreitol [DTT]). Recycled proteins were determined by subtracting remaining biotinylated protein from biotinylated protein detected after 10-min internalization.

Western blot analysis

After lysis, protein concentrations were analyzed with the Pierce (Rockford, IL) protein assay reagent. Samples were solubilized with LiCor sample buffer (LiCor, Lincoln, NE) with 400 mM DTT. Blots were blocked with LiCor blocking buffer and then probed with primary antibodies diluted in 0.05% Tween LiCor blocking buffer. Secondary antibodies were rabbit or mouse IR-Dye 680 or 800 in LiCor blocking buffer. Membranes were imaged using a LiCor Odyssey scanner. Boxes were manually placed around each band of interest, which returned near-infrared fluorescence values of raw intensity with intralane background subtracted using Odyssey 3.0 analytical software. The fluorescence value for each protein of interest was normalized to the in-lane value of β-actin, and this normalized ratio from duplicate or triplicate lanes was averaged. Data were analyzed using an unpaired *t* test. Measures were considered significant when $p < 0.05$. Error bars are SEM.

Cyst culture

Eight-well chamber slides were coated with 10 µl/well Matrigel, and cells (1000 cells/well) were added. Added to each well was 200 µl of media with 2% Matrigel. For quantification of lumen formation, cysts were fixed and labeled with antibodies against gp135 (podocalyxin) and E-cadherin after 4 d in culture. Cysts were quantified using a 20× objective and counted as single-lumen or multilumen cysts.

Statistical analysis

Western blots, TER, and morphological data were quantified as described. Data are presented as mean ± SEM. Graphical presentation of results and statistical analysis were carried out using Excel (Microsoft, Redmond, WA). Error bars are SEM, and significance values were calculated using a two-tailed unpaired *t* test at a 95% confidence interval.

ACKNOWLEDGMENTS

We thank members of the Wilson and Ghosh labs for helpful discussions. This work was supported by National Institutes of Health Grant DK084047.

REFERENCES

Akhtar N, Streuli CH (2013). An integrin-ILK-microtubule network orients cell polarity and lumen formation in glandular epithelium. Nat Cell Biol 15, 17–27.

Amasheh M, Fromm A, Krug SM, Amasheh S, Andres S, Zeitz M, Fromm M, Schulzke JD (2010). TNFalpha-induced and berberine-antagonized tight junction barrier impairment via tyrosine kinase, Akt and NFkappaB signaling. J Cell Sci 123, 4145–4155.

Anderson JM, Van Itallie CM (2009). Physiology and function of the tight junction. Cold Spring Harb Perspect Biol 1, a002584.

Apodaca G, Gallo LI, Bryant DM (2012). Role of membrane traffic in the generation of epithelial cell asymmetry. Nat Cell Biol 14, 1235–1243.

Bagnat M, Cheung ID, Mostov KE, Stainier DY (2007). Genetic control of single lumen formation in the zebrafish gut. Nat Cell Biol 9, 954–960.

Bruewer M, Hopkins AM, Hobert ME, Nusrat A, Madara JL (2004). RhoA, Rac1, and Cdc42 exert distinct effects on epithelial barrier via selective structural and biochemical modulation of junctional proteins and F-actin. Am J Physiol Cell Physiol 287, C327–C335.

Bryant DM, Datta A, Rodriguez-Fraticelli AE, Peranen J, Martin-Belmonte F, Mostov KE (2010). A molecular network for de novo generation of the apical surface and lumen. Nat Cell Biol 12, 1035–1045.

Datta A, Bryant DM, Mostov KE (2011). Molecular regulation of lumen morphogenesis. Curr Biol 21, R126–R136.

Desclozeaux M, Venturato J, Wylie FG, Kay JG, Joseph SR, Le HT, Stow JL (2008). Active Rab11 and functional recycling endosome are required for E-cadherin trafficking and lumen formation during epithelial morphogenesis. Am J Physiol Cell Physiol 295, C545–C556.

Dukes JD, Whitley P, Chalmers AD (2012). The PIKfyve inhibitor YM201636 blocks the continuous recycling of the tight junction proteins claudin-1 and claudin-2 in MDCK cells. PLoS One 7, e28659.

Elbediwy A, Zihni C, Terry SJ, Clark P, Matter K, Balda MS (2012). Epithelial junction formation requires confinement of Cdc42 activity by a novel SH3BP1 complex. J Cell Biol 198, 677–693.

Furuse M, Furuse K, Sasaki H, Tsukita S (2001). Conversion of zonulae occludentes from tight to leaky strand type by introducing claudin-2 into Madin-Darby canine kidney I cells. J Cell Biol 153, 263–272.

Galvez-Santisteban M *et al.* (2012). Synaptotagmin-like proteins control the formation of a single apical membrane domain in epithelial cells. Nat Cell Biol 14, 838–849.

Gumbiner B, Stevenson B, Grimaldi A (1988). The role of the cell adhesion molecule uvomorulin in the formation and maintenance of the epithelial junctional complex. J Cell Biol 107, 1575–1587.

Hou J, Gomes AS, Paul DL, Goodenough DA (2006). Study of claudin function by RNA interference. J Biol Chem 281, 36117–36123.

Iden S, Misselwitz S, Peddibhotla SS, Tuncay H, Rehder D, Gerke V, Robenek H, Suzuki A, Ebnet K (2012). aPKC phosphorylates JAM-A at Ser285 to promote cell contact maturation and tight junction formation. J Cell Biol 196, 623–639.

Ishikura S, Bilan PJ, Klip A (2007). Rabs 8A and 14 are targets of the insulin-regulated Rab-GAP AS160 regulating GLUT4 traffic in muscle cells. Biochem Biophys Res Commun 353, 1074–1079.

Ivanov AI, Nusrat A, Parkos CA (2005). Endocytosis of the apical junctional complex: mechanisms and possible roles in regulation of epithelial barriers. Bioessays 27, 356–365.

Kitt KN, Hernandez-Deviez D, Ballantyne SD, Spiliotis ET, Casanova JE, Wilson JM (2008). Rab14 regulates apical targeting in polarized epithelial cells. Traffic 9, 1218–1231.

Kohler K, Louvard D, Zahraoui A (2004). Rab13 regulates PKA signaling during tight junction assembly. J Cell Biol 165, 175–180.

Krishnan M, Lapierre LA, Knowles BC, Goldenring JR (2013). Rab25 regulates integrin expression in polarized colonic epithelial cells. Mol Biol Cell 24, 818–831.

Kuijl C *et al.* (2007). Intracellular bacterial growth is controlled by a kinase network around PKB/AKT1. Nature 450, 725–730.

Kyei GB, Vergne I, Chua J, Roberts E, Harris J, Junutula JR, Deretic V (2006). Rab14 is critical for maintenance of *Mycobacterium tuberculosis* phagosome maturation arrest. EMBO J 25, 5250–5259.

Lapierre LA, Avant KM, Caldwell CM, Oztan A, Apodaca G, Knowles BC, Roland JT, Ducharme NA, Goldenring JR (2012). Phosphorylation of Rab11-FIP2 regulates polarity in MDCK cells. Mol Biol Cell 23, 2302–2318.

Linford A, Yoshimura S, Nunes Bastos R, Langemeyer L, Gerondopoulos A, Rigden DJ, Barr FA (2012). Rab14 and its exchange factor FAM116 link endocytic recycling and adherens junction stability in migrating cells. Dev Cell 22, 952–966.

Lock JG, Stow JL (2005). Rab11 in recycling endosomes regulates the sorting and basolateral transport of E-cadherin. Mol Biol Cell 16, 1744–1755.

Marchiando AM *et al.* (2010). Caveolin-1-dependent occludin endocytosis is required for TNF-induced tight junction regulation in vivo. J Cell Biol 189, 111–126.

Marzesco AM, Dunia I, Pandjaitan R, Recouvreur M, Dauzonne D, Benedetti EL, Louvard D, Zahraoui A (2002). The small GTPase Rab13 regulates assembly of functional tight junctions in epithelial cells. Mol Biol Cell 13, 1819–1831.

Momose F, Sekimoto T, Ohkura T, Jo S, Kawaguchi A, Nagata K, Morikawa Y (2011). Apical transport of influenza A virus ribonucleoprotein requires Rab11-positive recycling endosome. PLoS One 6, e21123.

Morimoto S, Nishimura N, Terai T, Manabe S, Yamamoto Y, Shinahara W, Miyake H, Tashiro S, Shimada M, Sasaki T (2005). Rab13 mediates the continuous endocytic recycling of occludin to the cell surface. J Biol Chem 280, 2220–2228.

O'Brien LE, Jou TS, Pollack AL, Zhang Q, Hansen SH, Yurchenco P, Mostov KE (2001). Rac1 orientates epithelial apical polarity through effects on basolateral laminin assembly. Nat Cell Biol 3, 831–838.

Pieczynski J, Margolis B (2011). Protein complexes that control renal epithelial polarity. Am J Physiol Renal Physiol 300, F589–F601.

Roeth JF, Sawyer JK, Wilner DA, Peifer M (2009). Rab11 helps maintain apical crumbs and adherens junctions in the Drosophila embryonic ectoderm. PLoS One 4, e7634.

Rojas R, Ruiz WG, Leung SM, Jou TS, Apodaca G (2001). Cdc42-dependent modulation of tight junctions and membrane protein traffic in polarized Madin-Darby canine kidney cells. Mol Biol Cell 12, 2257–2274.

Schluter MA, Pfarr CS, Pieczynski J, Whiteman EL, Hurd TW, Fan S, Liu CJ, Margolis B (2009). Trafficking of Crumbs3 during cytokinesis is crucial for lumen formation. Mol Biol Cell 20, 4652–4663.

Senga K, Mostov KE, Mitaka T, Miyajima A, Tanimizu N (2012). Grainyhead-like 2 regulates epithelial morphogenesis by establishing functional tight junctions through the organization of a molecular network among claudin3, claudin4, and Rab25. Mol Biol Cell 23, 2845–2855.

Shen L (2012). Tight junctions on the move: molecular mechanisms for epithelial barrier regulation. Ann NY Acad Sci 1258, 9–18.

Shin K, Fogg VC, Margolis B (2006). Tight junctions and cell polarity. Annu Rev Cell Dev Biol 22, 207–235.

Suzuki T, Yoshinaga N, Tanabe S (2011). Interleukin-6 (IL-6) regulates claudin-2 expression and tight junction permeability in intestinal epithelium. J Biol Chem. 286, 31263–31271.

Thompson BJ (2013). Cell polarity: models and mechanisms from yeast, worms and flies. Development 140, 13–21.

Ueno H, Huang X, Tanaka Y, Hirokawa N (2011). KIF16B/Rab14 molecular motor complex is critical for early embryonic development by transporting FGF receptor. Dev Cell 20, 60–71.

Van Itallie CM, Tietgens AJ, LoGrande K, Aponte A, Gucek M, Anderson JM (2012). Phosphorylation of claudin-2 on serine 208 promotes membrane retention and reduces trafficking to lysosomes. J Cell Sci 125, 4902–4912.

Wallace SW, Durgan J, Jin D, Hall A (2010). Cdc42 regulates apical junction formation in human bronchial epithelial cells through PAK4 and Par6B. Mol Biol Cell 21, 2996–3006.

Weber CR, Nalle SC, Tretiakova M, Rubin DT, Turner JR (2008). Claudin-1 and claudin-2 expression is elevated in inflammatory bowel disease and may contribute to early neoplastic transformation. Lab Invest 88, 1110–1120.

Yamamura R, Nishimura N, Nakatsuji H, Arase S, Sasaki T (2008). The interaction of JRAB/MICAL-L2 with Rab8 and Rab13 coordinates the assembly of tight junctions and adherens junctions. Mol Biol Cell 19, 971–983.

Yu W, Datta A, Leroy P, O'Brien LE, Mak G, Jou TS, Matlin KS, Mostov KE, Zegers MM (2005). Beta1-integrin orients epithelial polarity via Rac1 and laminin. Mol Biol Cell 16, 433–445.

Zeissig S, Burgel N, Gunzel D, Richter J, Mankertz J, Wahnschaffe U, Kroesen AJ, Zeitz M, Fromm M, Schulzke JD (2007). Changes in expression and distribution of claudin 2, 5 and 8 lead to discontinuous tight junctions and barrier dysfunction in active Crohn's disease. Gut 56, 61–72.